Mon. Not. R. Astron. Soc. **000**, 000–000 (0000) Printed 3 April 2009 (MN LATEX style file v2.2)

The formation and survival of discs in a ΛCDM universe

Cecilia Scannapieco [1⋆], Simon D.M White[1], Volker Springel[1] and Patricia B. Tissera[2,3]
[1] *Max-Planck Institute for Astrophysics, Karl-Schwarzchild Str. 1, D85748, Garching, Germany.*
[2] *Instituto de Astronomía y Física del Espacio, Casilla de Correos 67, Suc. 28, 1428, Buenos Aires, Argentina.*
[3] *Consejo Nacional de Investigaciones Científicas y Técnicas, CONICET, Argentina.*

3 April 2009

ABSTRACT

We study the formation of galaxies in a Λ cold dark matter (ΛCDM) universe using high resolution hydrodynamical simulations with a multiphase treatment of gas, cooling and feedback, focusing on the formation of discs. Our simulations follow eight isolated haloes similar in mass to the Milky Way and extracted from a large cosmological simulation without restriction on spin parameter or merger history. This allows us to investigate how the final properties of the simulated galaxies correlate with the formation histories of their haloes. We find that, at $z = 0$, none of our galaxies contain a disc with more than 20 per cent of its total stellar mass. Four of the eight galaxies nevertheless have well-formed disc components, three have dominant spheroids and very small discs, and one is a spheroidal galaxy with no disc at all. The $z = 0$ spheroids are made of old stars, while discs are younger and formed from the inside-out. Neither the existence of a disc at $z = 0$ nor the final disc-to-total mass ratio seems to depend on the spin parameter of the halo. Discs are formed in haloes with spin parameters as low as 0.01 and as high as 0.05; galaxies with little or no disc component span the same range in spin parameter. Except for one of the simulated galaxies, all have significant discs at $z \gtrsim 2$, regardless of their $z = 0$ morphologies. Major mergers and instabilities, which arise when accreting cold gas is misaligned with the stellar disc, trigger a transfer of mass from the discs to the spheroids. In some cases, discs are destroyed, while in others, they survive or reform. This suggests that the survival probability of discs depends on the particular formation history of each galaxy. A realistic ΛCDM model will clearly require weaker star formation at high redshift and later disc assembly than occurs in our models.

Key words: galaxies: formation - evolution - cosmology: theory - methods: numerical

1 INTRODUCTION

According to the standard picture of cosmic structure formation, dark matter and baryons acquire similar specific angular momentum during their collapse through external torques from neighbouring structures (Hoyle 1953; Peebles 1969; White 1984). Discs are formed as the gas cools and condenses within the dark matter haloes conserving its specific angular momentum (White & Rees 1978; Fall & Efstathiou 1980; Mo, Mao & White 1998). In these models, the final properties of discs are closely linked to those of their parent haloes: for example, disc sizes and stability properties depend on the spin parameter of the dark matter haloes in which they reside.

However, discs are unstable against rapid changes in the gravitational potential, such as those produced by the accretion of satellites (Toth & Ostriker 1992; Quinn, Hernquist & Fullagar 1993; Velazquez & White 1999). Mergers of gas-poor disc galaxies are expected to produce early-type galaxies as remnants (Toomre & Toomre 1972; Toomre 1977). Isolated galaxy mergers have been extensively studied with hydrodynamical simulations, confirming that major mergers can indeed transform disc galaxies into elliptical-like systems (Barnes 1992; Barnes & Hernquist 1992, 1996; Mihos & Hernquist 1994, 1996). Given the fragility of discs and the fact that hierarchical models predict mergers to occur quite frequently, the existence of present-day spiral galaxies has been interpreted as an indirect proof of late disc formation in systems with a quiescent recent past.

Numerical hydrodynamical simulations are a powerful tool to study galaxy formation and evolution in its full cosmological context, since mergers are then naturally ac-

⋆ E-mail: cecilia@mpa-garching.mpg.de

counted for. State-of-the-art simulations currently include treatments of star formation, cooling, chemical enrichment and supernova (SN) feedback, and in some cases other processes such as black hole formation, active galactic nuclei (AGN) feedback and/or cosmic ray generation. These have been successful in reproducing some observed properties of galaxies, such as overall scaling relations, star formation histories and chemical abundances (e.g. Springel & Hernquist 2003; Brook et al. 2004; Okamoto et al. 2005; Oppenheimer & Davé 2006; Stinson et al. 2006; Governato et al. 2007; Dalla Vecchia & Schaye 2008; Dubois & Teyssier 2008; Finlator & Davé 2008; Scannapieco et al. 2008 (hereafter S08); among recent examples). However, such simulations have generally had difficulty reproducing disc-dominated galaxies in typical dark matter haloes, when taking into account the cosmological setting. A major problem is known as the "angular momentum catastrophe". This occurs when baryons condense early and then transfer a significant fraction of their angular momentum to the dark matter as the final galaxy is assembled (Navarro & Benz 1991; Navarro & White 1994). As a result, discs contain too small a fraction of the stellar mass in comparison to observed spirals.

In a limited number of cases, simulations have been able to produce individual examples of realistic disc galaxies in Λ cold dark matter (ΛCDM) universes (e.g. Abadi et al. 2003; Governato et al. 2004; Robertson et al. 2004; Okamoto et al. 2005; Governato et al. 2007; S08; see also Croft et al. 2008). Though, none has produced a viable late-type spiral. These simulations use the 'zoom' technique which allows an individual galaxy to be simulated at high resolution in its proper cosmological context. The relative success of these models appears to reflect the inclusion of efficient supernova feedback and improved numerical resolution. Typically, the simulated haloes are chosen so as to improve the chances of disc formation: masses similar to the Milky Way, relatively high spin parameters, and quiet merger histories. Such haloes are believed to be the most likely to produce disc galaxies, but given our incomplete knowledge of galaxy formation and evolution, and our repeated failure to reproduce late-type spirals, it is uncertain whether these assumptions are correct.

In a recent paper (S08), we studied the effects of SN feedback on the formation of galaxy discs by using cosmological simulations of a Milky Way-type galaxy. This study used an extension of the Tree-PM SPH code GADGET-2 (Springel 2005) which includes star formation, chemical enrichment and SN feedback, metal-dependent cooling and a multiphase model for the gas component (Scannapieco et al. 2005, 2006; hereafter S05, S06 respectively). Unlike other schemes, this treatment does not require ad hoc elements such as suppression of cooling after SN explosions or the explicit insertion of winds. Galactic winds are *naturally* generated when the multiphase gas model and SN feedback are included. In S08, we showed that this model can produce realistic discs from cosmological initial conditions. This is a consequence of self-regulation of the star formation and the generation of galactic winds. Most combinations of the input parameters yield disc-like components, although with different sizes and thicknesses, indicating that the code can form discs without fine-tuning the implemented physics. In all cases tested, however, the dominant stellar component by mass was the spheroid.

In this paper, we investigate these issues further by following the evolution of eight different galaxy-halo systems in a ΛCDM universe at higher resolution than in our previous work. We use an updated simulation code GADGET-3 (Springel et al. 2008) which includes our multiphase gas and feedback algorithms. Target haloes, similar in mass as the Milky Way and mildly isolated, were chosen from a dark matter only simulation of a cosmological volume, with no restriction on their spin parameter or merger history. These haloes were resimulated including baryons and at improved mass and force resolution. Our main goal here is to test whether realistic discs form in typical ΛCDM haloes and whether spin parameter or merger history influences their properties as usually assumed.

Our paper is organized as follows. In Section 2, we describe the main characteristics of the initial conditions and the implemented physics. In Section 3, we present the properties of our simulated galaxies at $z = 0$, while in Section 4, we investigate the relation between the present-day morphology of the galaxies and the properties of their parent dark matter haloes. In Section 5, we study the evolution of discs with time and investigate the processes leading to a morphological transformation. Finally, in Section 6, we summarize our main results.

2 METHODOLOGY

In this section, we describe the initial conditions used for our study, as well as the simulation code and the implemented physics. We also summarize previous results which led us to the input parameters assumed in our simulations.

2.1 Initial conditions and simulation setup

In this paper, we study a set of eight galaxy-sized haloes which were selected as part of the Aquarius Project of the Virgo Consortium (Springel et al. 2008). Target haloes were chosen at $z = 0$ from a simulation of a cosmological box of 137 Mpc on a side. New initial conditions were then constructed with improved mass resolution. The initial conditions originally had dark matter particles only because the main Aquarius Project studies the properties of the dark matter distribution. Gas particles were added to these initial conditions for our simulations, displaced by half the interparticle separation, and the mass of dark matter particles was reduced accordingly. We refer to Springel et al. (2008) for a detailed explanation of the generation of the initial conditions. Target haloes were chosen to have similar mass as the Milky Way and to be mildly isolated at $z = 0$ (no neighbour exceeding half of their mass within 1.4 Mpc). Except for these conditions, the haloes were selected randomly from the parent simulation.

Our simulations follow the evolution of matter from $z = 127$ to $z = 0$ in a ΛCDM universe with the following cosmological parameters: $\Omega_\Lambda = 0.75$, $\Omega_\mathrm{m} = 0.25$, $\Omega_\mathrm{b} = 0.04$, $\sigma_8 = 0.9$ and $H_0 = 73$ km s^{-1} Mpc^{-1}. The masses of dark matter and gas particles used in each simulation are listed in Table 1. We have adopted the same gravitational softening

for dark matter, gas and star particles, which varies in the range $0.7 - 1.4$ kpc for the different simulations[1].

The simulated galaxies have $z = 0$ virial masses in the range $\sim 7 - 16 \times 10^{11}$ $M_\odot$ and are represented by about 1 million particles within their virial radius. At $z = 0$, baryon fractions are about 0.10 within this radius, which are smaller than the global value of 0.16, indicating that a significant amount of baryons has been lost through winds. The main characteristics of the haloes, at $z = 0$, are listed in Table 1. We show the virial radius (r_{200}) and virial mass (M_{200}), the masses in stars and in gas within the virial radius, the optical radius ($r_{\rm opt}$, defined to enclose 83 per cent of the cold gas plus stellar mass), the baryon fraction within r_{200}, and the spin parameter, calculated using Eq. (5) of Bullock et al. (2001) at r_{200}. Following the convention of Springel et al. (2008) for halo naming, each of our haloes has a reference letter ("A" to "H") and a number (5 for all our simulations) which denotes the resolution level. Our sample includes the six haloes studied in Springel et al. (2008), and two additional ones. All of them were selected according to the same criteria.

In Table 1, we also show results for two lower resolution versions of simulation Aq-E-5. We find that the three Aq-E simulations give convergent results within a few per cent for the global properties of the galaxies (virial radius, virial mass, spin parameter). However, larger differences are detected for the final stellar mass, in particular for Aq-E-7. The lowest and intermediate resolution runs, at $z = 0$, respectively formed 45 and 10 per cent less stellar mass than the reference Aq-E-5 simulation. These results suggest that the main set of simulations presented in this paper have converged reasonably well (see also Section 3.)

2.2 The simulation code and implemented physics

The simulations analysed in this paper were run with an extended version of the code GADGET-3, an optimized version of GADGET-2 (Springel & Hernquist 2002; Springel 2005). GADGET-3 is a lagrangian-based code which uses a Tree-PM solver for the gravitational physics and the Smoothed Particle Hydrodynamics (SPH) technique for the gasdynamics. Our model includes a treatment for star formation and supernova feedback, as well as metal-dependent cooling and a multiphase model for the gas component. Here, we describe the main characteristics of our implementation, and we refer the interested reader to S05 and S06 for details. We note that our implementation of star formation and feedback is different from that of Springel & Hernquist (2003), although we do use their treatment for a UV background, based on the formulation of Haardt & Madau (1996).

2.2.1 Star formation

We assume that gas particles are eligible to form stars if they are denser than a threshold density ($\rho_{\rm th} = 7 \times 10^{-26}$ g cm^{-3}) and if they lie in a convergent flow. For these particles, we assume a star formation rate (SFR) per unit volume equal to

$$\dot{\rho}_\star = c \, \frac{\rho}{\tau_{\rm dyn}}, \qquad (1)$$

where c is the star formation efficiency, ρ and ρ_* are the gas and stellar densities, respectively, and $\tau_{\rm dyn} = 1/\sqrt{4\pi G \rho}$ is the local dynamical time of the gas. The star formation efficiency c sets the efficiency at which stars are formed or, equivalently, the typical time-scale of the star formation process. From gas particles eligible for star formation, stars are created stochastically (Springel & Hernquist 2003), and a maximum of two star particles are allowed to form from each gas particle.

2.2.2 Cooling

We use metal-dependent cooling functions (Sutherland & Dopita 1993) which take into account the dependence of cooling on the gas metallicity. We have a series of seven tables which correspond to different metallicities, from primordial to [Fe/H]= 0.5, from which we interpolate as needed. The inclusion of such metal-dependent cooling functions is important, since it has been shown that neglecting metals can lead to significant overestimation of the gas cooling times (e.g. S05; Kobayashi, Springel & White 2007).

2.2.3 Chemical enrichment

We include a treatment for the generation of Type II and Type Ia SN explosions (SNII and SNIa, respectively). For both types of events we compute, at each time-step, the number of exploding stars as well as the corresponding chemical production. For SNII, the number of exploding stars is calculated by convolving a Salpeter initial mass function (with lower and upper cut-offs of 0.1 and 40 $M_\odot$) with a metal-dependent life-time for massive stars (Raiteri, Villata & Navarro 1996) and assuming that SNII are generated by stars more massive than 8 $M_\odot$. For SNIa, we instead assume a rate of 0.3 relative to SNII (van den Bergh 1991) and a life-time taken randomly for each star within the interval $\tau_{\rm SNIa} = [0.7, 2]$ Gyr. We use the Woosley & Weaver (1995) chemical yields for SNII, which are metal-dependent and vary with relative metal abundances, and those of Thielemann, Nomoto & Hashimoto (1993) for SNIa. Chemical elements are distributed to the SPH neighbours of exploding stars, with a weight given by the smoothing kernel. Thereafter, there is no further mixing.

2.2.4 Multiphase gas model

We include a multiphase model for the gas component in order to avoid the artificial overcooling common in standard SPH codes (Thacker et al. 2000; Pearce et al. 2001). This model *decouples* particles with dissimilar properties, preventing them from being SPH neighbours. In practice, we *decouple* a given particle j from particle i, meaning that j is explicitly excluded from the neighbour list of i, if the following conditions are fulfilled:

$$A_i > \alpha A_j \qquad (2)$$

and

[1] Different simulations have been run with slightly different softenings. We have, however, performed a number of experiments to test the effects of varying the adopted softening within this range, and found that the results are not sensitive to this choice.

Table 1. Principal characteristics of the simulated haloes, at $z = 0$: virial radius ($r_{\rm vir}$), virial mass ($M_{\rm vir}$), mass in stars ($M_{\rm stars}$) and gas ($M_{\rm gas}$), optical radius ($r_{\rm opt}$), spin parameter (λ') calculated using Eq. (5) of Bullock et al. (2001) and baryon fraction. We also show the dark matter and gas particle masses.

Galaxy	$r_{\rm vir}$ [kpc]	$M_{\rm vir}$ [10^{10}M$_\odot$]	$M_{\rm star}$ [10^{10}M$_\odot$]	$M_{\rm gas}$ [10^{10}M$_\odot$]	$r_{\rm opt}$ [kpc]	λ'	$f_{\rm b}$	$m_{\rm DM}$ [10^6M$_\odot$]	$m_{\rm gas,0}$ [10^6M$_\odot$]
Aq-A-5	231.9	149.2	9.00	4.63	17.9	0.017	0.09	2.6	0.56
Aq-B-5	180.5	71.1	3.96	1.67	17.7	0.031	0.08	1.5	0.29
Aq-C-5	237.4	160.7	10.8	3.56	16.0	0.012	0.09	2.2	0.41
Aq-D-5	233.4	149.0	7.89	3.21	14.8	0.019	0.07	2.3	0.22
Aq-E-5	205.9	107.5	8.42	2.61	10.6	0.026	0.10	1.8	0.33
Aq-F-5	195.8	91.2	7.70	1.68	14.1	0.049	0.10	1.2	0.23
Aq-G-5	179.6	68.1	4.40	1.53	14.1	0.048	0.09	1.2	0.23
Aq-H-5	181.8	73.5	6.48	0.52	10.4	0.008	0.10	1.4	0.25
Aq-E-6	206.4	106.9	7.42	2.71	11.8	0.027	0.10	7.4	1.41
Aq-E-7	200.5	99.72	4.73	2.67	12.8	0.031	0.07	20.8	3.97

$$\mu_{ij} < c_{ij} \qquad (3)$$

where α is a constant, A_i is the entropic function of particle i (Springel & Hernquist 2002), c_{ij} is the pair-averaged sound speed, and μ_{ij} measures the relative velocity of particles i and j projected on to their separation vector (Springel 2005). The latter condition is included to avoid decoupling in shock waves, which can lead to unphysical effects when particles on opposite sides of a shock do not see each other (Marri & White 2003).

This multiphase model has been designed to improve the description of hot, diffuse material in the context of the SPH technique. One of its major advantages over previous implementations is that no scale-dependent parameters are needed to get realistic behaviour and to generate outflowing winds from a wide variety of strongly star-forming systems. This treatment allows the coexistence of diffuse and dense gaseous components, and can be combined with a more effective scheme for injecting the energy and heavy elements from SNe into the distinct components of the interstellar medium (S06).

2.2.5 Feedback

We assume that each SN injects $E_{\rm SN} \times 10^{51}$ erg of *thermal* energy into the interstellar medium. At the time of a SN event, we calculate the total amount of energy produced by the star particle, and distribute it between its *cold* (temperature $T < T_{\rm crit} = 8 \times 10^4$ K and density $\rho > 0.1\rho_{\rm th}$) and *hot* (otherwise) gas neighbours. The fraction distributed into the cold neighbours is our so-called *feedback parameter* ϵ_c. The distribution of energy works differently for the different gas phases. Hot neighbours absorb the energy as thermal energy simultaneously with the SN explosions. Cold neighbours, instead, accumulate energy from successive SNe into a reservoir, and effectively receive it as thermal energy only after a time-delay, when the total accumulated energy is sufficient to raise the particle's entropy to a value similar to its *local hot* neighbours (see S06 for details). This procedure is coupled to the ejection of metals, which are distributed to the cold and hot phases in proportions, also set by the ϵ_c value, although enrichment always occurs simultaneously with the explosions.

2.3 Model advantages and input parameters

Our combined multiphase and SN feedback treatment is among the most detailed and least ad hoc models to study the formation of galaxies in a cosmological context so far developed. It does not include mass-dependent input parameters, and so is suitable for tracking the formation of systems with a wide range of properties from early times, when they were much smaller than today. The model adapts to different mass systems since both the hot and cold gas properties are locally determined by cooling, hydrodynamics and feedback at each time without reference to the global properties of the system. There is no need to include the ad hoc elements typically introduced in other schemes, such as cooling suppression after SN events, or "by-hand" wind generation. Our code, on the contrary, *naturally* generates galactic winds in galaxies of all masses, with a strength that reflects the depth of the corresponding potential well. This results in a unique tool to study the formation of galaxies in a cosmological context.

There are nevertheless input parameters related to the SN and multiphase gas models which need to be set. Recently, S08 carried out a series of simulations of a Milky Way-type halo varying the input parameters, and analysing the effects on galactic properties such as morphology, disc size, and disc and bulge mean ages. They found parameter ranges which produce galaxies of size and thickness similar to the Milky Way. Provided the input parameters are within these intervals, results are not very sensitive to their exact values.

The simulations presented in this paper were run using (almost) the same input parameters. We have used a star formation efficiency of $c = 0.1$, a decoupling parameter for the multiphase model of $\alpha = 50$ and a feedback parameter of $\epsilon_c = 0.5$. We used the same characteristics for the chemical model (explained above). The only parameter that was changed slightly between simulations was $E_{\rm SN}$, the energy input per SN, which was either 1 (for Aq-A-5, Aq-B-5 and Aq-D-5) or 0.7 (for Aq-C-5, Aq-E-5, Aq-F-5, Aq-G-5

and Aq-H-5), in units of 10^{51} erg. Although this variation might influence slightly the final properties of the simulated galaxies, it does not affect the overall results in a significant way.

3 PROPERTIES OF DISCS AND SPHEROIDS AT THE PRESENT TIME

In this Section, we study the main properties of the simulated galaxies. In particular, we investigate their morphologies, as well as their star formation histories. We also study separately the properties of the discs and spheroids, although in this paper we focus on the study of the discs, deferring a more detailed investigation of the spheroids to another paper.

In order to study the morphologies of the simulated galaxies at $z = 0$, we calculate the angular momentum of baryons in the inner regions of the haloes $\vec{J}$, and rotate the reference system in order to align $\vec{J}$ with the $z-$axis. Figs. 1 and 2 show maps of the stellar densities projected onto planes perpendicular and parallel to the z direction. Left-hand panels represent face-on views, whereas the middle and right-hand panels correspond to edge-on projections. The colours span 4 orders of magnitude in projected density, with brighter colours representing higher densities. Arrows trace the corresponding projected velocity fields. We find that the eight simulated galaxies present a variety of morphologies. It is striking that none of them has a dominant thin disc. About half of them do have substantial disc components, reflected both in the projected mass distributions and in their velocity fields, which display ordered rotation. An interesting feature is that, except for Aq-E-5, discs do not seem to extend to the innermost regions (see also below). Some of the simulated galaxies show little or no disc component, and no clear sign of ordered rotation around any axis. Also, we find that bars are present in most cases; the simulated galaxies are never perfectly axisymmetric.

In order to characterize the properties of the discs and spheroids formed in our simulations, we designed a procedure to segregate stars into two main components, which we refer to as *disc* and *spheroid*. This is similar to the method used in S08, but is improved in order to avoid contamination of the disc by spheroid stars, particularly in the central regions. Our procedure has a series of steps. First, we construct the distributions of the parameter ϵ of the simulated stars, defined as $\epsilon = j_z/j_{\rm circ}$, where j_z is the angular momentum of each star in the z-direction (i.e. the direction of $\vec{J}$), and $j_{\rm circ}$ is the angular momentum expected for a circular orbit at the same radius: $j_{\rm circ} = r \cdot v_{\rm circ}(r)$ (we use $v_{\rm circ}(r) = \sqrt{G\,M(r)/r}$, although the mass distribution is not spherically symmetric in the central regions). The parameter ϵ can be used to distinguish kinematically between stars in the disc and in the spheroid. In Fig. 3, we show its distribution for our simulated galaxies. We note that for this analysis, we only consider particles which belong to the main system within twice the optical radius, ignoring stars in satellites. The distributions typically show two peaks: one at $\epsilon_{\rm peak} \sim 1$ ($\epsilon_{\rm peak}$ changes slightly between galaxies) which is indicative of the presence of a disc in rotational support, and a second one at $\epsilon \sim 0$, corresponding to a spheroidal distribution dominated by velocity dispersion. We define $\epsilon_{\rm s}$ as the location of this peak, as indicated in Fig. 4. Note that $\epsilon_{\rm s} \sim 0$ for all simulations except Aq-E-5, where $\epsilon_{\rm s} \sim 0.45$, indicating that this spheroid has a substantial net rotation.

From the distribution of ϵ for the simulated galaxies, we can infer the relative importance of discs and spheroids. From our eight galaxies, four of them clearly have well-defined disc components (Aq-C-5, Aq-D-5, Aq-E-5 and Aq-G-5), three of them have dominant spheroids and small discs (Aq-A-5, Aq-B-5 and Aq-H-5), and one is a spheroidal system with no disc at all (Aq-F-5). Clearly, the ϵ distributions are useful to assign stars either to the disc or the spheroidal components. However, we find that a definition based on ϵ alone can lead to contamination of the discs by spheroid stars. We therefore looked for additional constraints that allow a better segregation of discs from spheroids. In Fig. 4, we show the distribution of ϵ as a function of projected distance in the disc plane (up to $1.5 \times r_{\rm opt}$) for our simulations. The colours represent the density of particles in each pixel. Clearly, there are typically two distinct components which populate different regions of this plane: disc stars ($\epsilon \sim 1$) are more extended in radius but do not seem to extend into the innermost regions, while spheroids are symmetrically located around $\epsilon \sim 0$ (except for Aq-E-5) and their stars are more concentrated within the central regions. We use this feature to help decide if stars belong to the disc component, by requiring disc stars to be located above the upper white lines shown in Fig. 4[2]. We also require disc stars to have orbits roughly contained in the disc plane. This is done by restricting disc stars to have $\cos\,\alpha > 0.7$, where α is the angle between the angular momentum of each star and $\vec{J}$. Stars which do not fulfil the conditions explained above are considered part of the spheroidal components. Note that the central regions of our galaxies are dominated by velocity dispersion (Fig. 4), so stars are present on all possible orbits. Our procedure avoids contamination of the disc by high ϵ stars in the central region, which more likely belong to the spheroidal component. Note that we define spheroid stars as those which are not part of the rotationally supported disc. As a result, spheroids will typically contain not only bulge and stellar halo stars, but also stellar bars, if they are present. For this paper, we prefer to have a clean definition of disc stars which is the main subject of this work. In a forthcoming paper, we will present a detailed study of the properties of the spheroidal components.

By using the disc-spheroid decomposition described above, we can study how the different components of our simulated galaxies formed, and how their stellar mass was assembled. In Fig. 5, we show the SFRs for our set of simulations. All of them show a similar behaviour, with an early starburst followed by a more quiescent star formation phase at recent times. The bursty shape found for the SFRs is characteristic of our SN feedback model (S06; S08). We also show the SFRs constructed separately from disc (green lines) and spheroid (red lines) stars. Clearly, both components have different typical time-scales of star formation; stars formed at early times contribute to the formation of spheroids, while recent star formation leads to the formation of discs. This can be quantified through the half-mass formation times

[2] See Appendix A for details in the disc-spheroid decomposition and in the procedure to construct the white lines.

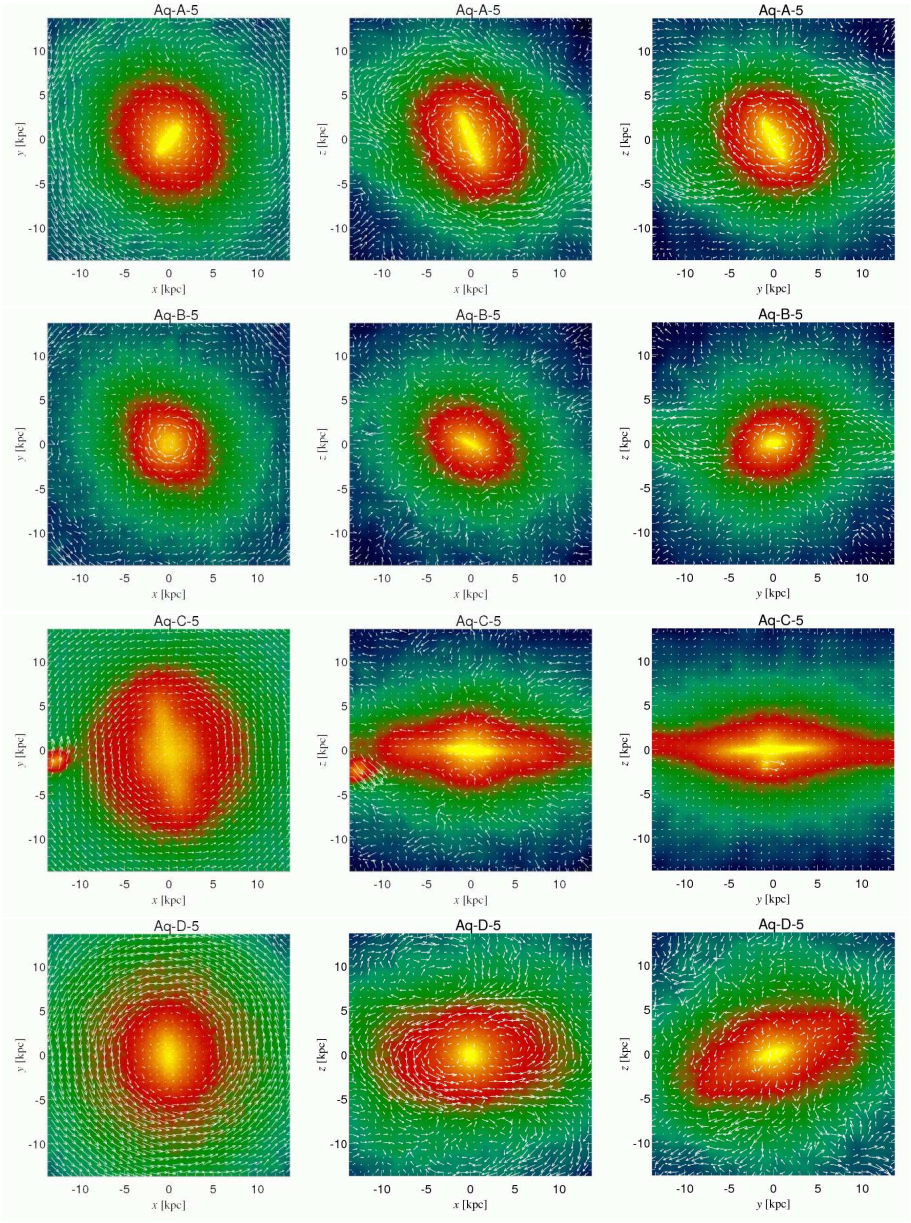

Figure 1. Face-on and edge-on stellar surface density maps for simulations Aq-A-5, Aq-B-5, Aq-C-5 and Aq-D-5 at $z = 0$. The colours span 4 orders of magnitude in projected stellar density, with brighter colours representing higher densities. The arrows trace the velocity field of the stars.

of the two components ($\tau_{\rm d}$ and $\tau_{\rm s}$), listed in Table 2. All spheroids are formed very early on, and they present typical mean formation times of the order of $\tau_{\rm s} \sim 1-3$ Gyr. In contrast, discs have younger stellar populations, with $\tau_{\rm d} \gtrsim 3-4$ Gyr in all cases.

In Table 2, we show the $z = 0$ masses of the discs and spheroids for the simulated galaxies. From these values, we can see that discs are substantially less massive than spheroids in all cases (see below). This suggests the need to prevent the formation of massive spheroids at early times: this would have the double effect of having less massive spheroids and leaving more gas available for star formation at recent times. It is striking that the remaining cold gas fractions in all our galaxies are very much smaller than in typical spiral galaxies. If more cold gas were left over, there would be a higher SFR at recent times, and later formation times for our discs, more similar to observed spirals (MacArthur et al. 2004). Possible solutions intended to prevent the formation of spheroids at early times and to retain more gas for later star formation in discs will be investigated in a separate work.

Our simulated galaxies have virial masses between 7×10^{11} and 1.6×10^{12} $M_\odot$. In order to quantify the prominence of the discs in each case, we have calculated the disc-to-total mass ratio D/T$\equiv M_{\rm d}/(M_{\rm d}+M_{\rm s})$, and the parameter $f_{\rm d,DM}$, defined as the ratio between disc mass and dark matter mass within the virial radius. The $f_{\rm d,DM}$ and D/T values obtained for our galaxies are shown in Table 2. Simulations Aq-C-5, Aq-D-5, Aq-E-5 and Aq-G-5 have the highest $f_{\rm d,DM}$ and D/T ratios, consistent with our results on their ϵ distribu-

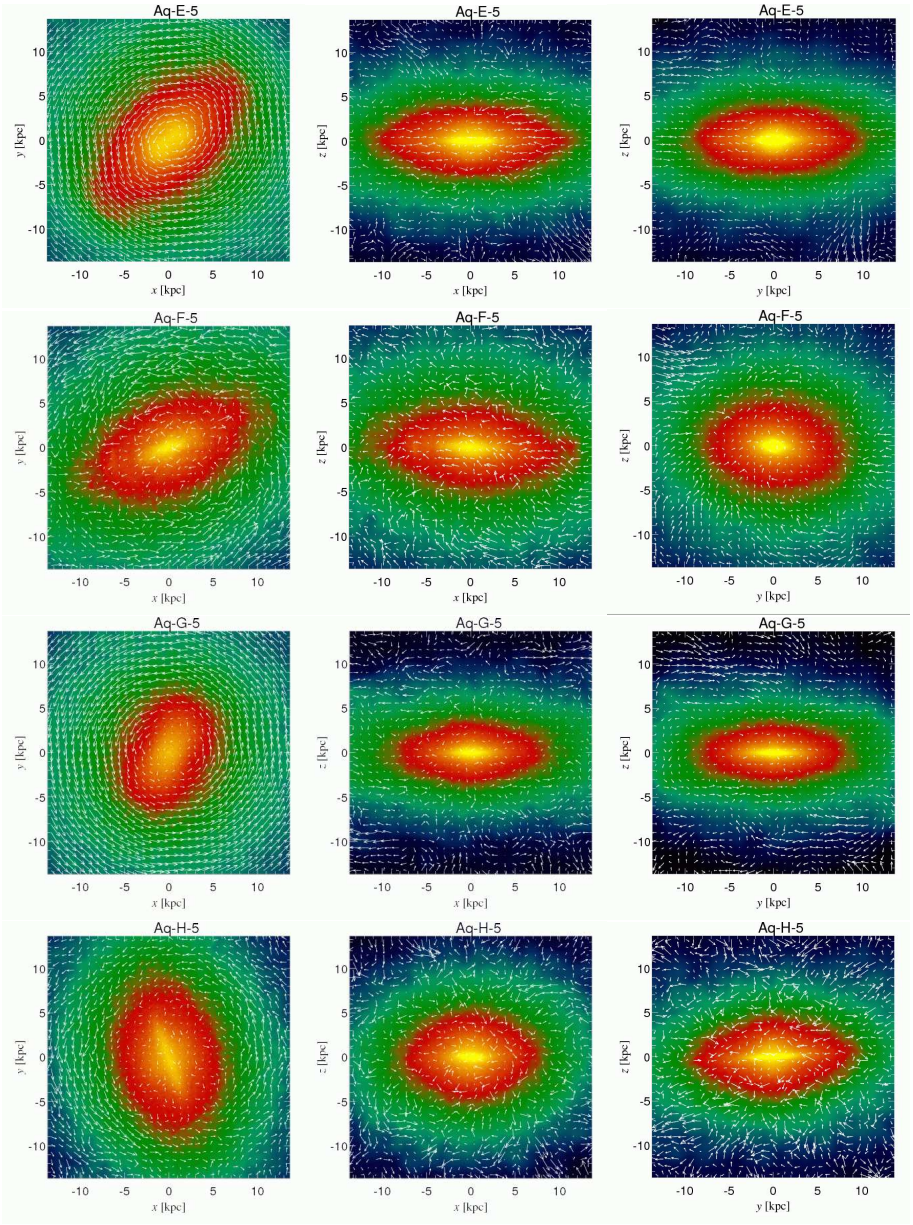

Figure 2. Face-on and edge-on stellar surface density maps for simulations Aq-E-5, Aq-F-5, Aq-G-5 and Aq-H-5 at $z = 0$. The colours span 4 orders of magnitude in projected stellar density, with brighter colours representing higher densities. The arrows trace the velocity field of the stars.

tions. In contrast, simulations with small discs are reflected in very small values of $f_{\rm d,DM}$ and D/T.

The D/T ratios obtained for our simulated galaxies, even for those with well-formed discs, are low in comparison with those of real spirals (e.g. Graham & Worley 2008). For comparison, the Milky Way has a disc-to-total ratio of 0.95. This indicates that, although our code is able to generate extended galaxy discs and does not suffer from catastrophic loss of angular momentum, the discs obtained from this "typical" set of initial conditions are much less massive than typical real discs. This is probably due to overly strong feedback which expels a significant amount of baryons from the systems and removes the new material for disc star formation. All systems have baryon fractions of $\lesssim 0.10$ (Table 1). As discussed above, our results suggest the need to investigate in more detail the formation of stars at early times which leads to the spheroidal components and the retention of cold disc gas to fuel recent star formation. The low SFRs we find in all our galaxies are a consequence of the very small amount of cold gas at low redshift, as indicated in Table 2.

We note, however, that a correct comparison with observations is not trivial. In particular, D/T ratios calculated from the simulations refer to stellar mass, not luminosity, and therefore do not consider the age of the stellar populations. Dust and inclination effects are not taken into account either. Also, our selection of disc stars based on their kinematics may exclude bars, for example, which are labeled as part of the spheroids. As a result, the D/T ratios listed in

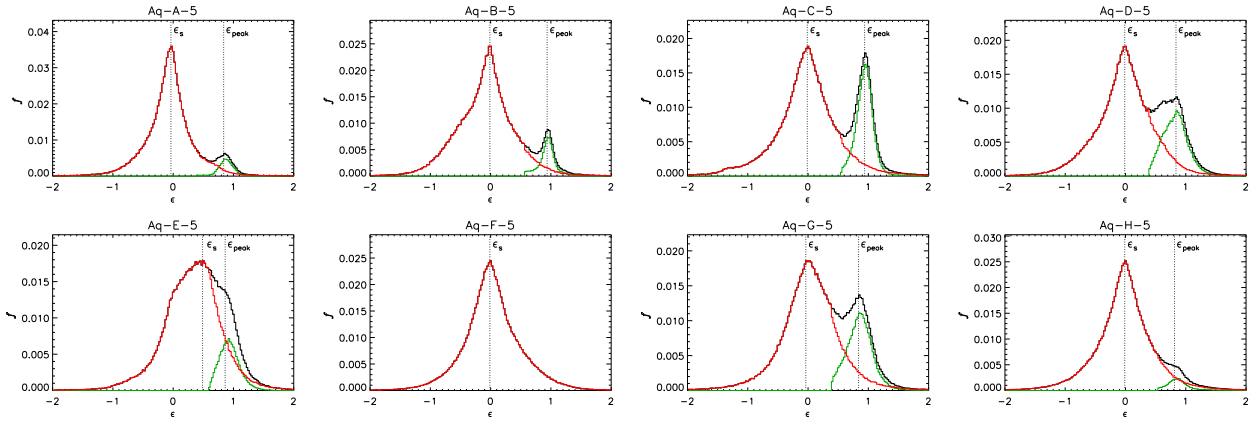

Figure 3. Stellar mass fraction as a function of $\epsilon = j_z/j_{\rm circ}$ for our set of simulations at $z = 0$ (black lines). Red and green lines correspond to the distributions for spheroid and disc stars, respectively, obtained with our disc-spheroid decomposition. We only consider stars which belong to the main system (i.e. we discount stars in satellites).

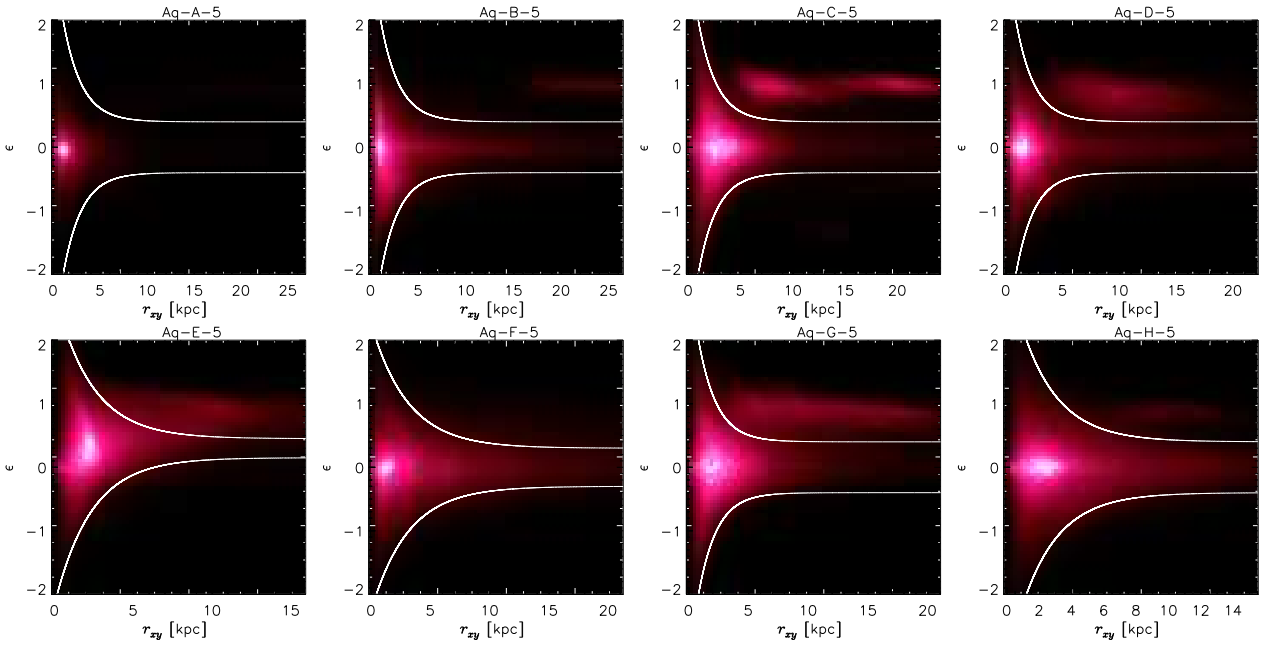

Figure 4. Eccentricity, $\epsilon = j_z/j_{\rm circ}$, as a function of radius in the disc plane for our set of simulations at $z = 0$. The colours scale with the density of points in each pixel, and brighter colours correspond to higher densities.

Table 2. Main properties of discs and spheroids obtained for the simulated galaxies: disc ($M_{\rm d}$) and spheroid ($M_{\rm s}$) masses, cold gas mass within twice the optical radius ($M_{\rm cold}$), ratio between disc and dark matter masses ($f_{\rm d,DM}$), disc-to-total mass ratio, half-mass formation times of discs ($\tau_{\rm d}$) and spheroids ($\tau_{\rm s}$), half-mass disc radius ($r_{\rm d}$) and half-mass height of disc stars ($h_{\rm d}$).

Galaxy	$M_{\rm d}$ [10^{10}M$_\odot$]	$M_{\rm s}$ [10^{10}M$_\odot$]	$M_{\rm cold}$ [10^{10}M$_\odot$]	$f_{\rm d,DM}$	D/T	$\tau_{\rm d}$ [Gyr]	$\tau_{\rm s}$ [Gyr]	$r_{\rm d}$ [kpc]	$h_{\rm d}$ [kpc]
Aq-A-5	0.55	8.45	0.151	0.004	0.061	7.63	1.73	21.2	0.42
Aq-B-5	0.34	3.62	0.033	0.005	0.087	8.51	3.38	24.0	0.14
Aq-C-5	2.30	8.48	0.118	0.016	0.213	4.47	1.29	12.2	0.81
Aq-D-5	1.60	6.29	0.001	0.012	0.204	4.92	2.19	11.0	2.95
Aq-E-5	1.12	7.10	0.044	0.012	0.136	2.90	2.23	12.9	1.89
Aq-F-5	-	7.70	0.009	-	-	-	2.89	-	-
Aq-G-5	1.03	3.37	0.060	0.017	0.234	4.63	1.98	10.82	1.85
Aq-H-5	0.29	6.19	0.011	0.004	0.044	3.66	1.56	10.56	5.14

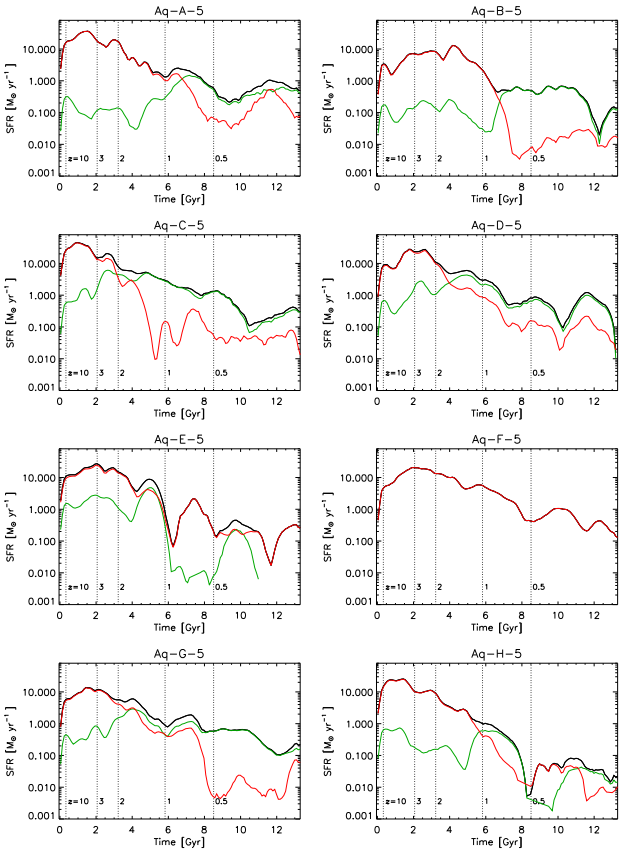

Figure 5. Star formation rates for our eight simulations. Black lines show the total SFRs, while green and red lines correspond to the SFRs of the discs and the spheroids, respectively.

Table 2 are probably underestimates of the mass of the geometrically thin component.

We note that although improved numerical resolution might help to produce more realistic and thinner discs, the failure to simulate the formation of late-type galaxies will not be solved by an increase in resolution. As mentioned above, we have tested the effects of resolution by running two lower resolution versions of Aq-E-5 (Table 1). In the case of Aq-E-6, we have also performed a full analysis of the final baryonic systems and find that the properties of the resulting discs and spheroids are consistent within a few per cent. This analysis suggests that the conclusions drawn from our level 5 resolution simulations are robust.

We have also calculated radial and vertical scale lengths for the discs in our simulations. Results are listed in Table 2, where we show the estimated half-mass radius ($r_{\rm d}$) and half-mass height ($h_{\rm d}$) for our discs. The radial extent of discs varies significantly between the simulations, but those with substantial discs all have similar size, $r_{\rm d} \sim 12$ kpc. Their thicknesses are more dissimilar, ranging over $0.8 - 3$ kpc.

We find that discs typically grow from the inside-out. As an example, in Fig. 6 we show the mean formation time of disc stars as a function of projected radius (green line) for simulation Aq-C-5. We also include results for the spheroidal component (red line). Dotted lines represent the $\pm\sigma$ scatter around the mean and dashed lines have been plotted at the times corresponding to $z = 1$ and $z = 0.5$. The vertical dotted line indicates the position of the optical radius. We find a clear trend between formation time and radius, indicating that the disc has grown from the inside out. This behaviour is common to all discs regardless of their size, except for Aq-E-5 where we find no trend between formation time and radius. Note that Aq-E-5 is the only galaxy in our sample where the spheroidal component has a net rotation. Even for those galaxies where the disc component is very small at $z = 0$ (such as Aq-A-5, Aq-B-5 and Aq-H-5), we find that discs formed from the inside-out. One interesting feature is that, in Aq-A-5 and Aq-B-5, the discs have very large half-mass radii $r_{\rm d} \gtrsim 21$ kpc and mean formation times $\tau_{\rm d} \sim 7.6$ Gyr (Table 2). These young discs are located farther from the centre, in comparison to the rest of our sample, even those with higher D/T ratios.

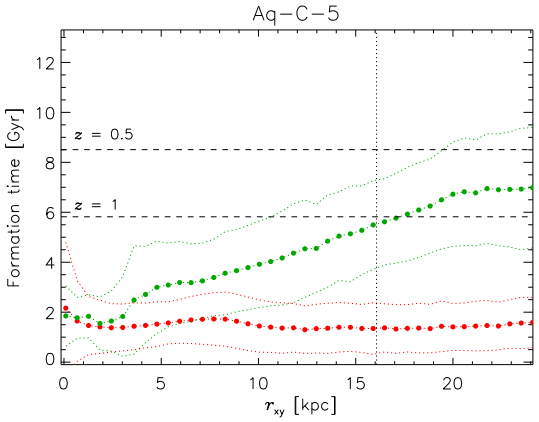

Figure 6. Mean formation time of disc (green lines) and spheroid (red lines) stars as a function of distance from the rotation axis, for simulation Aq-C-5. Dotted lines represent the $\pm\sigma$ scatter around the mean. The vertical line indicates the position of the optical radius of the galaxy, and horizontal lines have been drawn to indicate the times corresponding to $z = 1$ and $z = 0.5$.

The red line in Fig. 6 shows similar data for the spheroidal component. In this case, we find that the stars are all old, regardless of their distance from the centre of the galaxy. In all our galaxies (independent of the presence of a significant disc at $z = 0$), the spheroidal components are similar in terms of stellar age and spatial distribution. This suggests that the structure of spheroids is not very strongly affected by the presence of discs.

4 DISC FORMATION AND HALO PROPERTIES

So far, we have analysed the properties of discs and spheroids in our simulated galaxies. In this section, we look for hints to help us understand the relation between the morphology of galaxies and the properties of the dark matter haloes in which they reside.

First, we have investigated possible links between the presence of discs at $z = 0$ and the spin parameters λ' of the haloes, listed in Table 1. λ' has been calculated using Eq. (5) of Bullock et al. (2001) at the virial radius. In the left-hand panel of Fig. 7, we show the spin parameter of our haloes as a function of their virial masses. Spin parame-

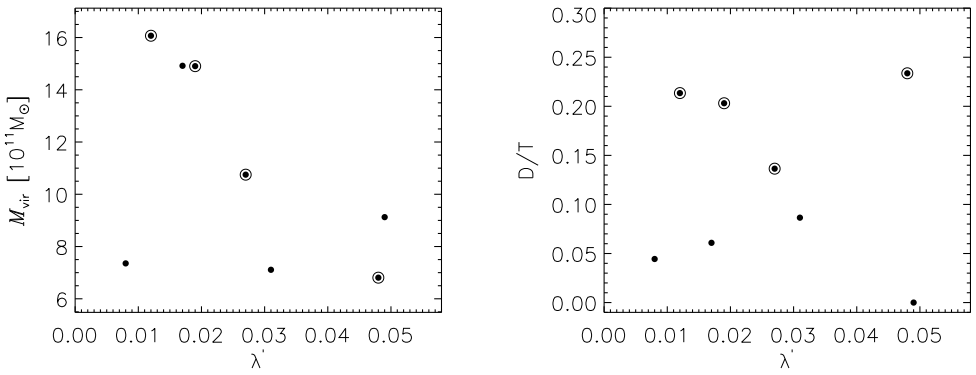

Figure 7. Virial mass (left-hand panel) and disc-to-total mass ratio (right-hand panel) for our simulated galaxies as a function of the spin parameter of their parent haloes. Encircled symbols correspond to galaxies with well-formed disc components at $z = 0$ (Aq-C-5, Aq-D-5, Aq-E-5 and Aq-G-5).

ters range between 0.008 and 0.05; and in this sample more massive haloes have lower spin parameters. Encircled symbols correspond to Aq-C-5, Aq-D-5, Aq-E-5 and Aq-G-5, the haloes where substantial disc components formed. We find no correlation between the spin parameter and the presence of significant discs at the present time. The right-hand panel of Fig. 7 shows the disc-to-total mass ratio of our galaxies as a function of their halo spin parameter. No trend is detected; in these simulations, discs have formed in haloes with spin parameters as high as $\lambda' \sim 0.05$ and as low as $\lambda' \sim 0.01$. Galaxies where discs are unimportant span the same range of spin parameters.

In Fig. 8, we show the specific angular momentum of the disc and spheroidal components as a function of the specific angular momentum of their dark matter halo. As above, encircled symbols correspond to those haloes where well-formed discs are present at $z = 0$. The dashed line indicates the identity relation. We find that spheroids have lower specific angular momenta than their dark matter haloes, as expected, but discs have high specific angular momenta, up to an order of magnitude larger than those of their dark matter haloes. We find this behaviour for all discs, regardless of their mass at the present time and of the spin parameter of their parent halo.

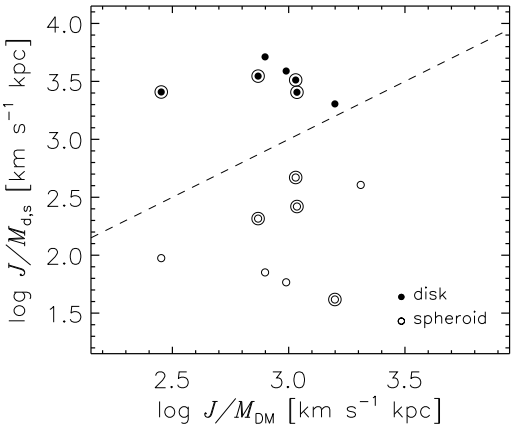

Figure 8. Specific angular momentum of the disc (filled symbols) and spheroidal (open symbols) components of simulated galaxies, as a function of specific angular momentum of the dark matter components. Encircled symbols correspond to galaxies with well-formed disc components at $z = 0$ (Aq-C-5, Aq-D-5, Aq-E-5 and Aq-G-5). The dashed line indicates the identity relation.

5 DISCS AT HIGH REDSHIFT AND DISC SURVIVAL

We find that all simulated galaxies, regardless of their D/T ratios at $z = 0$, were able to form discs at some time during their evolution. In order to quantify the relative importance of discs as a function of time, we have calculated the disc-to-total mass ratio at a series of redshifts for our simulated galaxies. In this case, we have not used the disc-spheroid decomposition described in Section 3; this method is quite time-consuming and requires inspection of the individual ϵ and density distributions. Instead, we have calculated D/T at each time assuming that the mass of the disc is given by the total mass of $\epsilon \geq 0.5$ stars. We find that this estimation gives slightly higher D/T ratios at $z = 0$ than those obtained with the disc-spheroid decomposition of Section 3. Because of this, we have shifted down the D/T ratios obtained in this way by a fixed factor f_s (f_s is different depending on the galaxy and it is independent of redshift), in order to recover, at $z = 0$, the $z = 0$ D/T ratios of Table 2. The f_s values are $\lesssim 0.1$ in all cases, except for Aq-E-5, where $f_s = 0.3$. In particular, we find that seven out of our eight simulated galaxies had significant disc components at $z \gtrsim 2$, and six of them at $z \sim 1$.

Fig. 9 shows the evolution with time of the D/T ratios for our eight simulated galaxies. We have divided the plot in such a way that galaxies with little or no disc components at $z = 0$ are in the left-hand panel, while galaxies with more prominent discs at the present time are in the right-hand one. Clearly, the relative importance of discs and spheroids at the present time has been reached in different ways. Let us first concentrate on those galaxies with little disc component at $z = 0$ (left-hand panel). It is clear that these

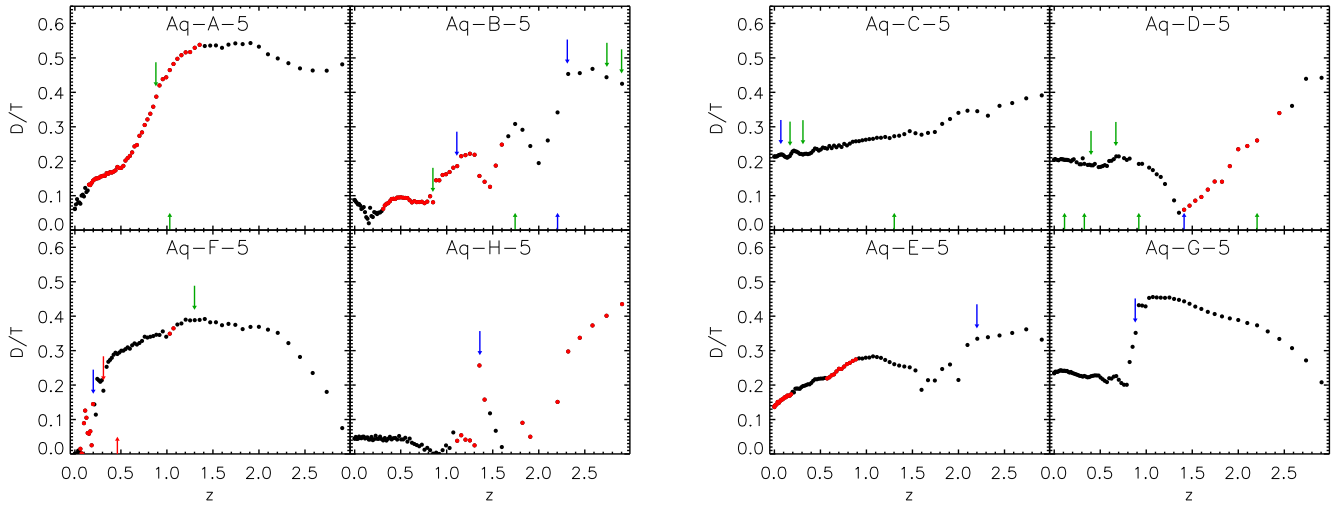

Figure 9. Disc-to-total mass ratio as a function of redshift for simulated galaxies. We have divided the plot in such a way that galaxies with little or no disc components at $z = 0$ are plotted in the left-hand panel, while galaxies with more prominent discs at the present time reside in the right-hand one. The arrows indicate the entrance of satellites either to the virial radius (upward arrows) or to the central (comoving) 27 kpc (downward arrows). Arrows are colour-coded according to the merger ratio $f \equiv M_{\rm sat}/M_{\rm cen}$: red, blue and green colours correspond to $f > 0.3$, $0.1 < f \leq 0.3$, and $0.02 < f \leq 0.1$, respectively. Red points indicate periods of strong misalignment between the cold gaseous and stellar discs: cos $\beta < 0.5$, see Fig. 10.

galaxies have discs at higher redshifts; discs did even dominate the stellar mass, such as in Aq-A-5. Later on, however, these discs transferred most of their mass to the spheroids, although in different ways. Aq-A-5 had a large disc which was quite stable until $z \sim 1$; after this time, its D/T ratio decreases steadily. A similar behaviour is found for Aq-F-5, the only galaxy of our sample with no disc component at $z = 0$. Aq-B-5 undergoes a series of sharp changes in its D/T ratio, and a new disc started to grow near $z = 0$. Finally, Aq-H-5 had a significant disc only at $z \gtrsim 2$ which dissolved by $z \sim 1$; after this time, a new disc formed, although it was not able to grow enough to produce a substantial component by $z = 0$.

The galaxies plotted in the right-hand panel of Fig. 9 did produce important discs by $z = 0$. Here, we also detect differences in the way discs formed. In Aq-C-5 and Aq-E-5, discs were present even at $z = 3$ and they remain stable until $z = 0$. Aq-D-5 had a significant disc at $z = 3$ that dissolved by $z \sim 1.5$, but a new disc formed between $z = 1.5$ and $z = 1$ which survived until the present time. Aq-G-5 had quite a massive disc at high redshift with a maximum D/T ratio of about 0.5 at $z \sim 1$; later, however, the disc starts losing mass to the spheroid to reach $z = 0$ with D/T ≈ 0.2.

Our findings suggest that discs are quite common at high redshift, but they often do not survive until the present time. The critical question is clearly what determines the survival or destruction of discs. It is generally thought that mergers and disc instabilities are the principal processes contributing to a change in galaxy morphology. Here, we investigate some features that affect the evolution of discs and spheroids in our simulated galaxies. On one hand, we investigate the effects of mergers on the disc components. On the other hand, we study whether misalignment between the gaseous and stellar discs can trigger instabilities which transfer mass from the discs to the spheroids.

Major mergers are known to destroy discs and to produce spheroidal remnants. In order to illustrate this effect, we have included in Fig. 9 two sets of arrows which show when satellites enter the inner 27 comoving kpc (downward arrows), or the virial radius (upward arrows). The arrows are colour-coded according to $f \equiv M_{\rm sat}/M_{\rm cen}$ where $M_{\rm sat}$ and $M_{\rm cen}$ are the stellar masses of the satellite and of the central object, respectively. We include only those events where $f > 0.02$. Red arrows indicate events with $f > 0.3$, blue arrows correspond to $0.1 < f \leq 0.3$, and green ones to $0.02 < f \leq 0.1$[3]. We define major mergers as those with $f > 0.3$ (red arrows). With this definition, only Aq-F-5 experiences a major merger ($f = 0.4$) which happens at $z \sim 0.5$, and completely destroys the disc. This galaxy is the only one in our sample that, at $z = 0$, has no disc component at all.

Mergers where $0.10 < f \leq 0.30$ can also produce important effects on the baryonic mass distributions. We find that, in some cases, such events coincide with a decrease in the D/T ratios, as is most clearly seen in the case of Aq-G-5. In this galaxy, the D/T ratio drops rapidly from ~ 0.45 to ~ 0.2 after a merger event (with $f = 0.17$); however, the disc is able to survive until $z = 0$. Smaller satellites ($f < 0.1$) do not seem to significantly affect the mass distributions. In general, we find that the effects of mergers with similar f values can be different for different galaxies, presumably this partly depends on the orbit of the infalling satellite. These results suggest that satellites may significantly affect

[3] In terms of total masses, we find lower values for the relative masses of the satellite and the central objects, this indicates that the dark matter is more strongly stripped than the stars.

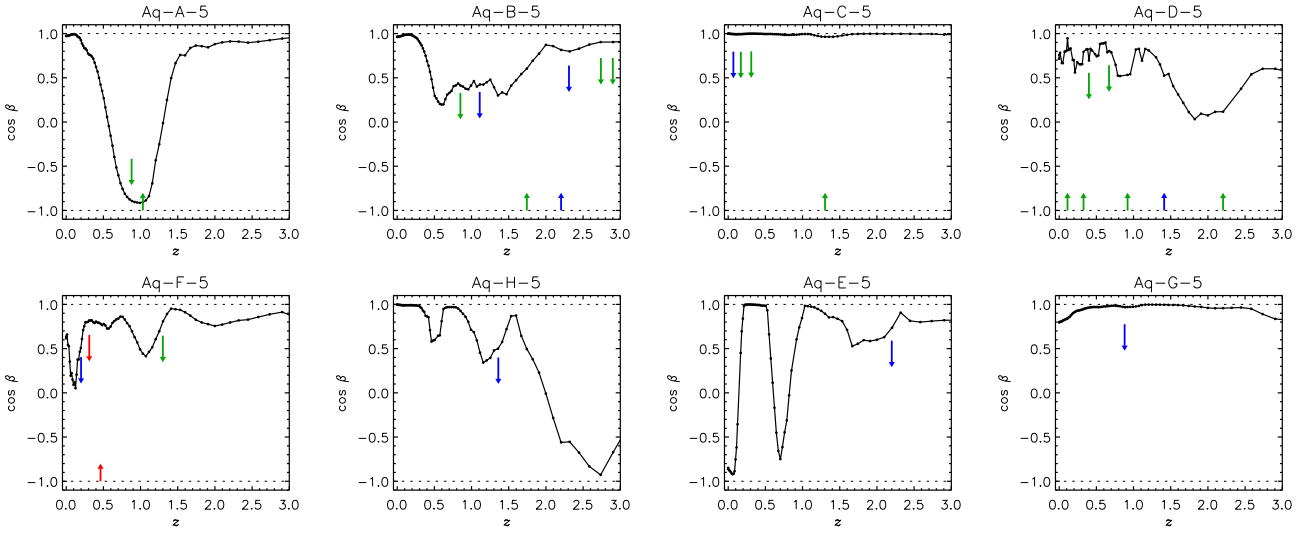

Figure 10. Cosine of the angle β between the angular momentum vectors of the cold gas and stars in the inner 27 comoving kpc as a function of redshift. The plot has been organized in such a way that galaxies with little or no disc component at $z = 0$ are plotted on the left panels, while galaxies with more prominent discs at the present time are on the right. Arrows indicate the entrance of satellites either within the virial radius (upward arrows) or within the central (comoving) 27 kpc (downward arrows). Arrows are colour-coded according to the merger ratio $f \equiv M_{\rm sat}/M_{\rm cen}$: red, blue and green colours correspond to $f > 0.3$, $0.1 < f \leq 0.3$, and $0.02 < f \leq 0.1$, respectively.

galaxy evolution, depending on both the relative mass of the satellite and central systems and the satellite's orbit.

We now investigate another process which can lead to the destruction or shrinking of discs, this is the misalignment between the angular momentum of infalling cold gas and that of the stars in the centre of galactic haloes. Infall of intergalactic or interstellar gas, as well as of satellites, can induce this behaviour. We find that misalignment between the gaseous and stellar discs is quite a common feature in our simulations, and can significantly contribute to the transfer of mass from the discs to the spheroids. In Fig. 10, we show the cosine of β, the angle between the angular momentum vector of the cold gas and that of the stars in the central region of the galaxies, as a function of redshift[4] The first two columns show results for Aq-A-5, Aq-B-5, Aq-F-5 and Aq-H-5, which have big spheroids and little discs at $z = 0$; whereas the last two columns correspond to Aq-C-5, Aq-D-5, Aq-E-5 and Aq-G-5, galaxies with more prominent discs. We find clear differences in the evolution of β for these two groups of galaxies. Those in the second group, which have significant disc components at $z = 0$, typically have cos $\beta\sim 1$ since $z = 3$ (except for Aq-D-5 where, around $z \sim 2$, the angular momenta of the cold disc and of the stars are almost perpendicular). (In the case of Aq-E-5, we detect two periods of misalignment corresponding to infalling cold clumps.) On the contrary, those galaxies in the first group (with little disc at $z = 0$) show significant and rapid changes in cos β with redshift. This indicates that the cold gas and stars are not coplanar. Note that a second stellar disc, not aligned with the already existing one, may be formed from the cold gas, provided it is dense enough. In some cases, the cold gas and stellar components are even roughly counter-rotating, such as in Aq-A-5 and Aq-B-5 at $z \sim 0.5$, and in Aq-H-5 at $z \gtrsim 2$.

The interaction between two misaligned discs destabilizes the systems, triggering a redistribution of mass from the discs to the spheroids. This can be seen in Fig. 9, where we have drawn in red those points where cos $\beta\leq 0.5$. Clearly, a high misalignment between the gaseous and stellar discs is always accompanied by a decrease in the D/T ratio, indicating that mass is being transferred from the disc to the spheroid. Note that, at high redshift, the decrease in D/T may also indicate that spheroids are getting more massive, not at the expense of the disc. However, for $z \lesssim 2$ there are almost no new spheroid stars, as can be inferred from the star formation rates of spheroid stars (Fig. 5) and from the spheroid half-mass formation times $\tau_{\rm s}$ (Table 2), and therefore D/T can only decrease if stellar mass from the discs is transferred to the spheroids.

Our results show that both major mergers and disc instability, where mass is transferred from discs to spheroids, contribute to the destruction and/or shrinking of discs. Taking into account the results of the previous section, we conclude that the presence of discs at $z = 0$ is more likely determined by the particular formation and merger histories of galaxies, rather than by the spin parameter of their parent haloes. The absence of major mergers seems to be a necessary condition for discs to form, but not to be sufficient.

6 CONCLUSIONS

We have used a series of simulations to study the formation of galaxies in a ΛCDM cosmology. Our simulations have enough resolution to follow the internal structure of galaxies and, at the same time, to keep track of larger scale processes

[4] We have used an arbitrary threshold radius of 20 $h^{-1} = 27$ comoving kpc. Provided most baryons are within this region, our results are not sensitive to this choice.

such as mergers, infall and tidal stripping. We have simulated the evolution of eight galaxies with virial masses in the range $7 - 16 \times 10^{11} M_\odot$. These were selected purely on the basis of their mass ($\sim 10^{12}$ $M_\odot$) and in isolation (no companion exceeding half of their mass within 1.4 Mpc), with no additional restriction on spin parameter or merger history. The only condition was the absence of close massive companions at $z = 0$. As a result, our sample, although still small, should be representative for the formation of isolated galaxies similar to the Milky Way.

Dark matter only simulations of these haloes with much higher resolution than those studied here have been carried out for the Aquarius Project of the Virgo Consortium (Springel et al. 2008). In this paper, we have included gas dynamics using a specialized extension of the code GADGET-3 which includes star formation and supernova feedback (both from Type II and from Type Ia SNe), metal-dependent cooling, a multiphase treatment of the gas component, and photoheating by the UV background (S05; S06). This hydrodynamical code includes no scale-dependent parameters, and is among the most detailed and least ad hoc attempts to describe the interstellar medium physics and SN feedback in galaxy formation. One of its main advantages is that galactic winds are naturally generated, without the ad hoc prescriptions required in most alternative simulation codes.

With the parameters adopted here, none of our eight haloes grows a $z = 0$ disc with more than about 20 per cent of the total stellar mass. Four of the simulated galaxies do have well-formed and substantial discs in rotational support, three have dominant spheroids and little discs, and one has no disc at all. The star formation histories of all galaxies are similar, with an early starburst followed by a more quiescent phase and little star formation at $z = 0$. Old stars populate the spheroids, while younger stars are found in the discs. As a result, typical half-mass formation times are $\tau_s \sim 1 - 3$ Gyr for spheroids and $\tau_d \gtrsim 4$ Gyr for discs. We find that, regardless of the presence or absence of a disc, all spheroids have similar mass profiles and stellar age distributions. While all discs formed from the inside-out, their mass distributions show greater variety.

Even the most massive discs formed in these simulations produce disc-to-total mass ratios of the order of 0.2, much lower than those of late-type spirals or of the Milky Way. This is primarily because of the small amount of cold gas available for star formation at late times. Presumably, this is either due to an excess of star formation at early times which leaves the systems with too little gas to make a large disc, or due to too efficient feedback which expels the gas which would otherwise make the disc. We will investigate this problem in more detail in a forthcoming paper.

We find that disc growth in dark matter haloes does not depend on spin parameter. We have significant discs in haloes with spin parameter as low as 0.01 and as high as 0.05, and galaxies with little or no disc component in haloes with the same range of spin parameters. We also find no relation between disc mass fraction and halo spin parameter.

As expected, our discs have high specific angular momentum, even higher than that of their dark matter haloes. In fact, the discs in our simulations all have similar specific angular momenta, independently of their mass. Spheroids, on the contrary, span a wide range of specific angular momentum, although in all cases their values are smaller than those of the parent dark matter haloes. Those spheroids with the highest specific angular momenta are found in haloes which have prominent discs at $z = 0$.

The variation of disc-to-total ratio with redshift reveals that all our galaxies were able to form discs at some time during their evolution. At high redshift, some discs are comparable in mass to their spheroids. However, discs often fail to survive until the present time. We find that both major mergers and misalignment between the discs and newly accreted gas can completely or partially destroy them. Only one of our galaxies experiences a major merger which completely destroys its disc and, at $z = 0$, it only has a spheroid. Misalignment between stellar discs and newly accreted cold gas is more frequent and induces instabilities which transfer a significant amount of mass from the discs to the spheroids. Among the galaxies which do have significant discs at $z = 0$, there are substantial differences in disc evolution. Discs can be stable since $z = 3$; they can be completely destroyed and can regrow; or they can lose part of their mass but survive until $z = 0$.

Our results suggest that discs can form easily in ΛCDM scenarios, regardless of the spin parameter of their parent haloes. However, their survival is strongly affected by major mergers and by disc instabilities. It is clear that the particular implementation of star formation and feedback physics in our current models, while it produces individual objects which resemble real galaxies, cannot produce a galaxy population which matches observation. In particular, the disc mass fractions of our simulated galaxies are typically much lower than those of real galaxies of similar stellar mass. We produce nothing which looks like the Milky Way or other late-type spirals. Apparently, real galaxies formed fewer stars at early times than our models and substantially more stars in a disc at late times.

ACKNOWLEDGMENTS

We thank the referee for his/her comments that helped improve the paper. The simulations were carried out at the Computing Centre of the Max-Planck-Society in Garching. This research was supported by the DFG cluster of excellence 'Origin and Structure of the Universe'. CS thanks A. Jenkins and A. Ludlow for generating the initial conditions used in this paper. This work was partially supported by PICT 32342 (2005), PICT Max-Planck 245 (2006) of Foncyt and the Secyt-DAAD bilateral collaboration (2007).

REFERENCES

Abadi M.G., Navarro J.F., Steinmetz M., Eke V.R., 2003, ApJ, 591, 499
Barnes J.E., 1992, ApJ, 393, 484
Barnes J.E., Hernquist L., 1992, ARA&A, 20, 705
Barnes J.E., Hernquist L., 1996, ApJ, 471, 115
Brook C.B., Kawata D., Gibson B.K., Flynn C., 2004, MNRAS, 349, 52
Bullock J.S., Dekel A., Kolatt T.S., Kravtsov A.V., Klypin A.A., Porciani C., Primack J.R., 2001, ApJ, 555, 240
Croft R.A.C, Di Matteo T., Springel V., Hernquist L., 2008, MNRAS (astro-p/0803.4003)
Dalla Vecchia C., Schaye J., 2008, MNRAS, 387, 1431

Dubois Y., Teyssier R., 2008, A&A, 477, 79
Fall S.M., Efstathiou, G., 1980, MNRAS, 193, 189
Finlator K., Davé R., 2008, MNRAS, 385, 2181
Governato F., et al., 2004, ApJ, 607, 688
Governato F., Willman B., Mayer L., Brooks A., Stinson G., Valenzuela O., Wadsley J., Quinn T., 2007, MNRAS, 374, 1479
Graham A.W., Worley C.C., 2008, MNRAS, 388, 1708
Haardt F., Madau P., 1996, ApJ, 461, 20
Hoyle F., 1953, ApJ, 118, 513
Kobayashi C., Springel V., White S.D.M., 2007, MNRAS, 376, 1465
MacArthur L.A., Courteau S., Bell E., Holtzman J.A., 2004, ApJS, 152, 175
Marri S., White S.D.M., 2003, MNRAS, 345, 561
Mihos J.C., Hernquist L., 1994, ApJ, 425, 13
Mihos J.C., Hernquist L., 1996, ApJ, 464, 641
Mo H.J., Mao S., White S.D.M., 1998, MNRAS, 295, 319
Navarro J.F., Benz W., 1991, ApJ, 380, 320
Navarro J.F., White S.D.M., 1994, MNRAS, 267, 401
Okamoto T., Eke V.R., Frenk C.S., Jenkins A., 2005, MNRAS, 363, 1299
Oppenheimer B.D., Davé R., 2006, MNRAS, 373, 1265
Pearce F.R., Jenkins A., Frenk C.S., White S.D.M., Thomas P.A., Couchman H.M.P., Peacock J.A., Efstathiou G., 2001, MNRAS, 326, 649
Peebles, P.J.E., 1969, ApJ, 155, 393
Quinn P.J., Hernquist L., Fullagar D.P., 1993, ApJ, 403, 74
Raiteri C.M., Villata M., Navarro J.F., 1996, A&A, 315, 105
Robertson B., Yoshida N., Springel V., Hernquist L., 2004, ApJ, 606, 32
Scannapieco C., Tissera P.B., White S.D.M., Springel V., 2005, MNRAS, 364, 552 (S05)
Scannapieco C., Tissera P.B., White S.D.M., Springel V., 2006, MNRAS, 371, 1125 (S06)
Scannapieco C., Tissera P.B., White S.D.M., Springel V., 2008, MNRAS, 389, 1137 (S08)
Springel V., Hernquist L., 2002, MNRAS, 333, 649
Springel V., Hernquist L., 2003, MNRAS, 339, 289
Springel V., 2005, MNRAS, 364, 1105
Springel V., et al., 2008, MNRAS, 391, 1685
Stinson G., Seth A., Katz N., Wadsley J., Governato F., Quinn T., 2006, MNRAS, 373, 1074
Sutherland R.S., Dopita M.A., 1993, ApJS, 88, 253
Thacker R.J., Tittley E.R., Pearce F.R., Couchman H.M.P., Thomas, P.A., 2000, MNRAS, 319, 619
Thielemann F. K., Nomoto K., Hashimoto M., 1993, in Prantzos N., Vangoni-Flam E., Cass N., eds, Origin and Evolution of the Elements. Cambridge Univ. Press, Cambridge , p. 299
Toomre A., 1977, ARA&A, 15, 437
Toomre A., Toomre J., 1972, ApJ, 178, 623
Toth G, Ostriker J.P., 1992, ApJ, 389, 5
van den Bergh S., 1991, ApJ, 369, 1
Velazquez H., White S.D.M., 1999, MNRAS, 304, 254
White S.D.M., 1984, ApJ, 286, 38
White S.D.M., Rees M.J., 1978, MNRAS, 183, 341
Woosley S. E., Weaver T. A., 1995, ApJS, 101, 181

APPENDIX A: DISC-SPHEROID DECOMPOSITION

In this Appendix, we explain in more detail the procedure we follow to assign stars to the disc and the spheroidal components. In particular, we explain how we construct the white curves shown in Fig. 4, which are used to avoid contamination of the disc by spheroid stars. Note that contamination will be present if the decomposition into the disc and spheroidal components is based on ϵ only. The most clear example is Aq-F-5, where 4 per cent of the stars have $\epsilon \gtrsim 1$ (compatible with disc dynamics). However, this system is a pure spheroid. All simulations would suffer from this contamination if no further restriction were done for disc stars.

As explained in the text, our disc-spheroid decomposition is based on three conditions: $\epsilon \sim \epsilon_{\rm peak}$, orbits roughly contained in the disc plane and disc stars lying above the white lines shown in Fig. 4. The white lines are constructed in the following way. (i) For each simulated galaxy, we first draw the lower white line, using the following functional form,

$$y = \epsilon_{\rm s} - C1 - \exp(-(r_{xy} - C2)/C3) \qquad \text{(A1)}$$

and choosing values for $C1$, $C2$ and $C3$ in order to enclose most $\epsilon < \epsilon_{\rm s}$ stars (> 90 per cent) between this line and a horizontal one at $\epsilon = \epsilon_{\rm s}$. (Note that $\epsilon < \epsilon_{\rm s}$ stars can be used as clean tracers of the spheroid.) The detailed shape of the curve is not important, provided it encloses most of the spheroid stars. The upper white line is then constructed by reflecting the lower line symmetrically about $\epsilon_{\rm s}$. The white lines thus delimit the spatial region of the velocity dominated spheroidal component. (ii) As a safety check, we calculate the properties of the resulting disc and spheroid stars (stellar age, metallicity, mass profile). Since the global properties of the disc and spheroidal components in our simulated galaxies are distinct and well-defined, contamination is easily detected. For example, if high ϵ stars in Aq-F-5 are identified as disc stars, they will in any case be old, metal-poor, and centrally concentrated. These stars have the same characteristics as the spheroidal component present in this simulation, and clearly belong to it, rather than to a disc. Our procedure is successful in avoiding this contamination. (iii) If contamination is detected, we adjust our white lines, and repeat (ii) until we get clean samples for the disc and spheroidal components.

Note that this procedure is valid provided the disc and spheroidal components have distinct and well-defined properties, which is the case for our simulated galaxies. We have tried a number of other ways to avoid contamination of the discs by spheroid stars, and found this particular one to be the most satisfactory one since it can be successfully applied to all our simulations, including Aq-E-5, where the decomposition is the hardest.